### Title
Thermal and photochemical oxidation of self-assembled monolayers on alumina particles exposed to nitrogen dioxide




### Journal
Physical Chemistry Chemical Physics, 13(2)

### ISSN
1463-9076 1463-9084



### Authors
Raff, Jonathan D
Szanyi, János
Finlayson-Pitts, Barbara J



### Publication Date
2011

### DOI
10.1039/c0cp01041c

Peer reviewed

# Thermal and photochemical oxidation of self-assembled monolayers on alumina particles exposed to nitrogen dioxide

**Jonathan D. Raff,†[a] János Szanyi[b] and Barbara J. Finlayson-Pitts*[a]**

*Received 30th June 2010, Accepted 24th September 2010*
**DOI: 10.1039/c0cp01041c**



Alumina is an important component of airborne dust particles as well as of building materials and soils found in the tropospheric boundary layer. While the uptake and reactions of oxides of nitrogen and their photochemistry on alumina have been reported in the past, little is known about the chemistry when organics are also present. Fourier transform infrared (FTIR) spectroscopy at ~23 °C was used to study reactions of $NO_2$ on $\gamma$-$Al_2O_3$ particles that had been derivatized using 7-octenyltrichlorosilane to form a self-assembled monolayer (SAM). For comparison, the reactions with untreated $\gamma$-$Al_2O_3$ were also studied. In both cases, the particles were exposed to water vapor prior to $NO_2$ to provide adsorbed water for reaction. As expected, surface-bound HONO, $NO_2^-$, and $NO_3^-$ were formed. Surprisingly, oxidation of the organic by surface-bound nitrogen oxides was observed in the dark, forming organo-nitrogen products identified as nitronates ($R_2C{=}NO_2^-$). Oxidation was more rapid under irradiation ($\lambda > 290$ nm) and formed organic nitrates and carbonyl compounds and/or peroxy nitrates in addition to the products observed in the dark. Mass spectrometry of the gas phase during irradiation revealed the production of NO, $CO_2$, and CO. These studies provide evidence for oxidation of organic compounds on particles and boundary layer surfaces that are exposed to air containing oxides of nitrogen, as well as new pathways for the formation of nitrogen-containing compounds on these surfaces.

## Introduction

Mineral dust mobilized by dust storms in arid regions constitutes the largest mass fraction of aerosols in the atmosphere.[1–3] Due to its abundance in the atmosphere, dust plays an important role in climate, visibility, and human health.[1–6] In addition, the high surface area associated with mineral dust, which is mainly comprised of $SiO_2$, $Al_2O_3$, and trace elements,[3] provides sites for heterogeneous reactions that can significantly alter the chemical composition and toxicity of the aerosols, and affects the gas-phase composition of the atmosphere through the adsorption of gases.[7] Building materials and soils have many components common to mineral dust,[8] and hence similar chemistry is expected on boundary layer surfaces.

Oxides of nitrogen are known to adsorb to and react on mineral oxides.[9–14] For example, it has long been recognized that $NO_2$ hydrolysis occurs on such surfaces to form surface nitrite and nitrate ions,[3,13,15–18] both of which photolyze to generate OH radicals and NO or $NO_2$.[17,19–23] This chemistry leads to the release of highly photochemically labile gases such as HONO, a major OH source in the troposphere.[24–27] Consistent with the results of laboratory studies, increased HONO levels have been measured during dust storms.[28] Organic compounds are also known to be taken up on airborne dust particles[4,9,29–31] and on building materials in the boundary layer,[32–37] and there is evidence that oxidation of organics occurs on these surfaces as well.[33,38,39]

A number of the well-known surface-bound nitrogen oxides such as nitrite and nitrate ions photolyze in the actinic region[24] above 290 nm to form $O^-$ radical anions, which react with water to generate OH radicals.[19,20] It has been shown in recent studies[39–41] that this generation of OH on the surface can lead to oxidation of adsorbed organics, *i.e.*, oxidation from the "bottom up" as compared to the commonly accepted mechanism of oxidation from the "top down" by gases such as $O_3$, OH and $NO_3$.[24,42–45] Given the simultaneous presence of organics and oxides of nitrogen on the surfaces of mineral dust, soils and building materials, it is likely that similar photochemically-driven oxidations of the adsorbed organics could occur from the "bottom up."

In the present work, self-assembled monolayers (SAM) of a terminal alkene, 7-octenylsilyl groups, were attached to alumina ($\gamma$-$Al_2O_3$) particles as a model system for organic coatings on suspended mineral dust and boundary layer surfaces. Aluminium oxide was chosen as a substrate because of its natural abundance in mineral dust[30] and building materials,[8,24] its affinity for nitrogen oxides, and the ease of functionalizing the $Al_2O_3$ surface with unsaturated organosilane self-assembled layers of known composition.[46,47] The surface reactions were studied using Fourier transform infrared spectroscopy, while mass spectrometry was used to monitor gas-phase products formed by photolysis. It is shown that the surface-bound organic layer is oxidized not only during irradiation, but surprisingly, also in the dark. The atmospheric implications of these unusual findings are discussed.

[a] *Department of Chemistry, University of California, Irvine, CA 92697-2025. E-mail: bjfinlay@uci.edu; Fax: (949) 824-2420; Tel: (949) 824-7670*
[b] *Institute for Interfacial Catalysis, Pacific Northwest National Laboratory, Richland, WA 99352*
† Currently at the School of Public and Environmental Affairs, Indiana University, Bloomington, IN 47405.

 

## Experimental

### Preparation of SAMs on alumina

Alumina ($\gamma$-$Al_2O_3$, Inframat Advanced Materials, 99.99 + %) was first heated to 475 °C for 12 h to remove organic impurities and immediately upon cooling, was derivatized with 7-octenylsilyl groups [$H_2C{=}CH(CH_2)_6SiO_3$], designated hereafter as C8=. A stirred suspension of 100 mg of $\gamma$-$Al_2O_3$ in 25 mL of hexadecane was reacted with 7-octenyltrichlorosilane (0.25 mL, Sigma-Aldrich, 96%). The solid was rinsed four times using HPLC grade dichloromethane followed by vigorous shaking and centrifugation to remove unreacted dissolved starting material, and then final centrifugation used to isolate the solid. The residual solvent was removed under a gentle stream of nitrogen followed by evacuation at $\sim 10^{-4}$ Torr for 3 h. The underivatized alumina powder was verified as consisting exclusively of the $\gamma$-phase by X-ray diffraction (XRD).

Brunauer-Emmett-Teller (BET) surface areas[48] of derivatized and underivatized $\gamma$-$Al_2O_3$ substrates were determined by measuring nitrogen adsorption with an Autosorb-1 surface area analyzer (Quantachrome Instruments). Functionalization of the alumina particles with C8= resulted in a 28% reduction in surface area, from 167 ± 3 to 121 ± 4 $m^2\ g^{-1}$ (2σ). The surface coverage of C8= on one gram of alumina was estimated using the surface area (*SA*) of untreated alumina powder and the fractional organic carbon content of the derivatized particles [$f_{OC}$ = 10.1 ± 0.3% (2σ), determined by thermogravimetric analysis] according to eqn (I),

$$\text{surface coverage (molecules cm}^{-2}) = \frac{f_{OC} \cdot m \cdot N_A}{MW_{C8=} \cdot SA} \quad \text{(I)}$$

where $N_A$ is Avogadro's number, $MW_{C8=}$ is the molecular weight of an octenylsilane group (187 g $mol^{-1}$), *m* is the mass of the alumina substrate (1 g), and *SA* is the surface area of a gram of derivatized substrate (121 $m^2$). This gives a surface coverage of $\sim 2 \times 10^{14}$ molecules $cm^{-2}$. The surface –OH concentration of $\gamma$-$Al_2O_3$ heated to 500 °C for 12 h, similar to the thermal pretreatment of alumina used here, has been reported[49] to be $3.6 \times 10^{14}$ $cm^{-2}$. Thus, approximately half of the surface –OH groups have the C8= functional groups and, although the organic coating reduces the gas-accessible alumina surface area, regions of incomplete coverage remain where gases are able to access the $Al_2O_3$ surface.

### FTIR/MS Measurements

Experiments were conducted in a vacuum system equipped with a Fourier transform infrared (FTIR) spectrometer and a mass spectrometer (MS).[17] Samples of alumina particles coated with SAMs were pressed into a fine tungsten grid and mounted on a copper sample holder that enables precise temperature control between cryogenic temperatures and > 1000 K. The sample holder is housed in a stainless steel cube connected to a gas-handling manifold. A quartz fiber optics cable is used to irradiate the sample with light from an externally mounted high pressure Hg-arc lamp (Spectra Physics, Oriel 100 W); a dichroic mirror placed between the lamp and the fiber optics assembly minimizes heating of the sample by infrared radiation from the lamp. The spectrum of the photolysis light source consists of wavelengths greater than 290 nm, with a maximum between 350 and 450 nm. The FTIR spectrometer (Nicolet Magna 740) is equipped with a liquid nitrogen-cooled Hg–Cd–Te detector. Single beam spectra of the background and those collected during the reaction were obtained from the average of 64 interferograms at a resolution of 4 $cm^{-1}$. The mass spectrometer (UTI 100C) is attached to the sample chamber *via* leak and gate valves and uses electron ionization (EI) with a quadrupole mass analyzer. This system allows for simultaneous monitoring of species adsorbed to the substrate *via* FTIR as well as gas-phase reactants and products using a leak valve. Samples were irradiated continuously during FTIR experiments and in 40 s intervals for experiments designed to detect gaseous photolysis products with mass spectrometry.

The relative intensity of the lamp emission as a function of wavelength was measured using a spectrofluorometer (FluoroLog, HORIBA Jobin-Yvon), and placed on an absolute intensity scale using the photoisomerization of 2-nitrobenzaldehyde to 2-nitrosobenzoic acid (Φ = 0.5) as a chemical actinometer.[50] Samples were prepared by mixing 0.5 g of $\gamma$-$Al_2O_3$ with 0.02 g of 2-nitrobenzaldehyde (Sigma-Aldrich, 98%), pressing ~10 mg of the mixture into a fine tungsten grid and then irradiating under the same conditions used in the $NO_x/H_2O/C8{=}/\gamma$-$Al_2O_3$ photochemistry experiments. Formation of nitrosobenzoic acid in the substrate was followed by FTIR. Using this method, the total absolute intensity over the 290–400 nm region was $2.2 \times 10^{19}$ photons $cm^{-2}\ s^{-1}$.

## Results

Fig. 1 shows the infrared spectrum of the C8= SAM on alumina using a spectrum of uncoated alumina as the background. The absorptions are similar to previous measurements of alkylsiloxane SAMs on silica.[51,52] The most prominent peaks at 2927 and 2858 $cm^{-1}$ are due to the asymmetric and symmetric C–H stretching modes [$\nu_{as}(CH_2)$ and $\nu_s(CH_2)$] of the C8= methylene groups, while weaker bands attributed to $CH_2$ scissoring vibrations of the methylene groups occur between 1470 and 1440 $cm^{-1}$.[53] The terminal alkene gives rise to a vinyl =C–H stretch at 3082 $cm^{-1}$ and a sharp band at 1643 $cm^{-1}$ from the C=C stretch.[53] There is also a

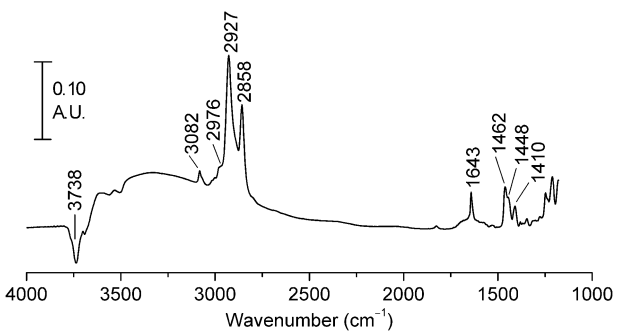


**Fig. 1** Fourier transform infrared spectrum of the C8= SAM on $\gamma$-$Al_2O_3$ powder using the underivatized powder as the background spectrum.

weak $=CH_2$ stretching vibration at 2976 $cm^{-1}$ and a band at 1410 $cm^{-1}$ from an in-plane deformation vibration (scissoring) of the $=CH_2$ group.[53] The disordered nature of the C8= chains in the SAM is revealed by the position and peak width of the $CH_2$ stretches shown in Fig. 1.[52,54] The $\nu_{as}(CH_2)$ of C8= on alumina particles at $\sim$2927 $cm^{-1}$ is shifted by +12 $cm^{-1}$ and the full-width at half maximum (fwhm) is $\sim$20 $cm^{-1}$ wider than the $\nu_{as}(CH_2)$ of a C18 alkane (ordered) film on a flat silica substrate.[52,54] A broad feature between 3600–2500 $cm^{-1}$ is likely due to small amounts of adsorbed water, while the sharp negative peak at 3738 $cm^{-1}$ is a surface O–H stretch[55] that decreases due to reaction with the C8= trichlorosilane groups. Additional decreases in surface –OH absorptions occur when the C8= SAM is exposed to water vapor (not shown), indicating that some surface –OH groups remain after coating and are available for interaction with gases.

Reactions of $NO_2$ on $\gamma$-$Al_2O_3$ particles with and without the C8= were first studied in the dark. Prior to sequential exposure of the sample to doses of $NO_2$, the $\gamma$-$Al_2O_3$ particles (either derivatized or untreated) were exposed to water vapor and subsequently evacuated for 30 min in order to provide surface-adsorbed water for the $NO_2$ hydrolysis. Chemisorption of nitrogen oxides on alumina is known to give a complex variety of adsorbed nitrite and nitrate species.[3,13,14,17,18,56,57] The amount of $NO_2$ that the substrate was exposed to was chosen to optimize the concentration of surface-adsorbed nitrite compared to nitrate. At higher $NO_2$ doses, nitrite is converted to nitrate *via* reaction (1):[17]

$$NO_2^-{}_{(ads)} + NO_{2(g)} \rightarrow NO_3^-{}_{(ads)} + NO_{(g)} \qquad (1)$$

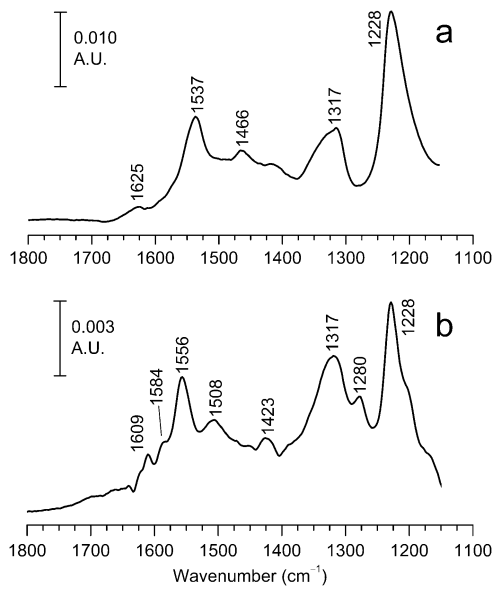


**Fig. 2** (a) Infrared spectrum of $\gamma$-$Al_2O_3$ after exposure to $H_2O$ and followed by addition of 45 mTorr $NO_2$; (b) spectrum of C8= derivatized $\gamma$-$Al_2O_3$ that was previously exposed to $H_2O$ after addition of 45 mTorr $NO_2$. Both spectra used the single beam spectrum just before the addition of $NO_2$ as the reference so that only changes due to the $NO_2$ reactions are seen.

Fig. 2a shows the spectrum of an underivatized alumina sample in the presence of $NO_2$. The spectrum is referenced to the single beam spectrum just before the addition of $NO_2$, so the observed changes are due solely to the uptake and reactions of the gas. Based on previous studies of species formed from exposure of $Al_2O_3$ to $NO_2$,[3,12–14,17,18,56–59] the peaks at 1625, 1537, and 1317 $cm^{-1}$ are assigned to surface-bound $NO_3^-$, and that at 1466 to surface-bound $NO_2^-$. The strongest peak at 1228 $cm^{-1}$ is assigned to surface-bound HONO.[17] This assignment is supported by previous observations of the formation of HONO on $Al_2O_3$,[17] by its loss during photolysis (see below) and by an accompanying broad weak peak near 3500 $cm^{-1}$ in the O–H stretching region (not shown), which is expected for HONO.[60,61]

Fig. 2b shows the analogous spectrum for the C8= SAM on alumina exposed to $NO_2$. Peaks due to HONO (1228 $cm^{-1}$) and $NO_3^-$ (1317, 1556 $cm^{-1}$) are again formed but are less intense as expected if the $Al_2O_3$ was partially protected by the SAM. New peaks appear at 1280, 1423, 1508, 1584, and 1609 $cm^{-1}$, and there are small decreases in peaks in the 3000 $cm^{-1}$ region due to losses of $CH_2$ and $=CH_2$ groups (not shown). The region of the spectrum between 1100 and 1600 $cm^{-1}$ is quite congested with absorptions due to nitrate bound in various ways to the surface (monodentate, bidentate and bridging).[12,17,56] However, the new peaks at 1280, 1584, and 1609 $cm^{-1}$ are only observed in the presence of the organic, and track each other with time (*i.e.*, their ratios remain constant), suggesting that they are due to organic products formed by reaction of surface-bound oxides of nitrogen with the C8= moiety.

After the spectrum in Fig. 2b was obtained, the cell was pumped out and spectra were collected over time to monitor the sample's stability in the dark under vacuum. Fig. 3a shows the changes in the spectra over the course of an hour. The peak due to surface HONO (at 1228 $cm^{-1}$) decreases and peaks at 2262, 1607, 1584, 1528, 1425, 1280, and 1165 $cm^{-1}$ grow in. While the reaction is slow, it is remarkable that it occurs in the dark at all. The small peak at 2262 $cm^{-1}$ is too small to follow quantitatively, but it appears to also be associated with peaks due to the organic products.

Fig. 3b shows the changes of the sample in Fig. 3a during irradiation with filtered light ($\lambda$ > 290 nm) over a period of 7 h. A partial pressure of 100 mTorr of $O_2$ was maintained to propagate alkoxy and peroxy radical pathways that occur under atmospheric conditions.[24] The spectra are the ratio of the single beam spectra of the C8= derivatized alumina/$H_2O$/$NO_x$ sample at various irradiation times to that of the sample prior to irradiation. Loss of surface-bound HONO and the formation of product peaks that are similar to those formed in the dark (Fig. 3a) are observed, but appear at a faster rate. A comparison of the rates of increase in the intensity of the peak at 1280 $cm^{-1}$ and loss of the peak at 1228 $cm^{-1}$ shows that the photochemical reactions are enhanced by a factor of two relative to those occurring in the dark. In addition, there is an intense peak at 1638 $cm^{-1}$ that we assign to an organic nitrate ($RONO_2$),[53] a peak at 1700 $cm^{-1}$ (discussed below), and a broad peak around 3200 $cm^{-1}$ assigned to adsorbed water.[52] The shape

 

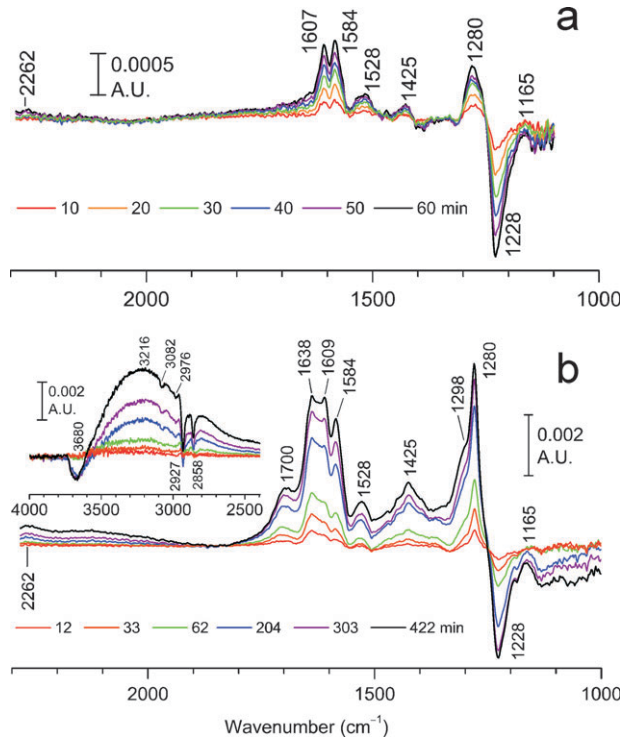


**Fig. 3** (a) Changes in the infrared spectrum of the SAM-coated $Al_2O_3$ that had been reacted with $NO_2$ (Fig. 2b) after pumping out the $NO_2$. The reference is the first spectrum taken after evacuating the cell, so that changes due to the thermal reaction in the dark are seen; (b) changes in the spectrum of the sample in (a) during photolysis ($\lambda > 290$ nm, $P_{O_2} = 100$ mTorr). The reference spectrum was taken immediately before irradiation to emphasize changes due to photolysis.

of the peaks in the 1550–1700 cm$^{-1}$ region suggests there is also an underlying broad peak, likely due to the bending vibration in water. Peaks due to –$CH_2$– and =$CH_2$ decrease, but it is noteworthy that the loss of $CH_2$ is large relative to loss of the =C–H stretch, suggesting that reaction of the double bond is not the sole, nor necessarily the primary reaction pathway. The negative peak at 3680 cm$^{-1}$ is due to a loss of free surface –OH groups that become involved in hydrogen bonding with water formed during photolysis.

The gas phase products generated during photolysis of C8= derivatized alumina that had been exposed to $H_2O/NO_2$ were monitored using mass spectrometry. Fig. 4a shows that during irradiation, gas phase products with peaks at $m/z$ 30, 44 and 28 were formed. It is noteworthy that there was no detectable peak at $m/z$ 46; however, the mass spectrum of an authentic sample of $NO_2$ under these conditions did not have a strong peak at $m/z$ 46, so that its yield in the present case is uncertain. While these peaks cannot be assigned with certainty with low resolution mass spectrometry, it is likely that they are due to NO, $CO_2$ and CO, respectively. A significant contribution from HCHO at $m/z$ 30 and 28 is ruled out by the absence of a peak at $m/z$ 29.[62] These gases are not observed when the sample is heated (+0.7 K) in the dark (see Fig. 4b, between 400–600 s), so the evolution of NO, $CO_2$, and CO is not an artifact of the substrate being heated (+0.3 K) during irradiation.

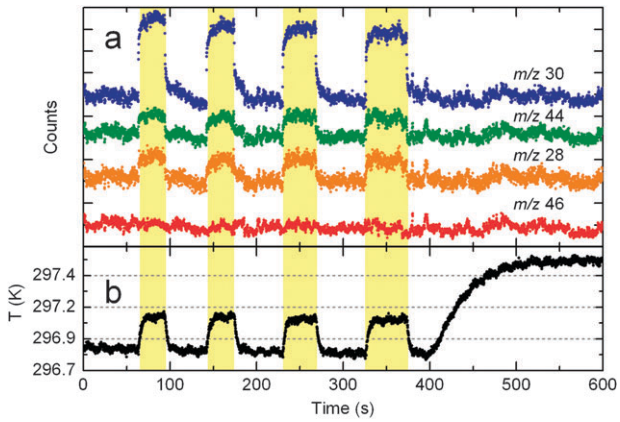


**Fig. 4** (a) Changes in peaks in mass spectrum at $m/z$ 30 (NO), 28 (CO), 44 ($CO_2$) and 46 ($NO_2$) induced by photolysis (yellow bars) at $\lambda > 290$ nm of a C8= SAM on $\gamma$-$Al_2O_3$ that was previously exposed to $H_2O$ and $NO_2$. (b) Changes in the sample temperature during photolysis. The sample is irradiated here in 40 s intervals to demonstrate repeatability of the measurement.

## Discussion

While there have been a number of studies of the uptake and reactions of $NO_2$ on alumina both in the absence and presence of water,[3,12–15,17,18,56–59,63] we are unaware of any study in which a SAM-derivatized alumina substrate was exposed to $NO_2$. Although perfectly ordered SAMs may provide an effective barrier between the gas-phase and the substrate, previous studies have shown that gases may penetrate between the hydrocarbon chains,[64,65] especially at the edges of defects and islands of a rough substrate. The C8= coverage is expected to be irregular on $Al_2O_3$ particles, exposing more of the substrate to gases compared to well-organized alkane SAMs on silica or gold, for example. In addition, as discussed above the surface concentration of the C8= SAM corresponds to approximately 50% of the initial available surface –OH groups on the $Al_2O_3$. This partial coverage, combined with the positions and widths of the –$CH_2$– bands indicating the SAM is relatively disordered, suggests that the $Al_2O_3$ surface will be accessible to the $NO_2$ after derivatization.

When $NO_2$ is taken up by a surface, particularly on metal oxides such as $Al_2O_3$, surface ions are formed,

$$2\ NO_2 \rightarrow NO^+NO_3^- \qquad (2)$$

where the $NO^+$ becomes associated with the surface oxide anions and the $NO_3^-$ with the surface aluminium cations. In the gas phase, water aids in this ionization[66] and the same is likely true on surfaces. In addition, water reacts with the $NO^+NO_3^-$ ion pair to form nitrous and nitric acids:[16,67–70]

$$NO^+NO_3^- + H_2O \rightarrow HONO + HNO_3 \qquad (3)$$

Nitrous acid can dissociate on the oxide surface to generate nitrite ions,

$$HONO \rightarrow H^+ + NO_2^- \qquad (4)$$

just as $HNO_3$ dissociates to form $NO_3^-$. Under sufficiently acidic conditions, protonation to generate $NO^+$ also occurs:

$$HONO + H^+ \rightarrow NO^+ + H_2O \quad (5)$$

Reactions (2)–(5) are consistent with the formation of surface-bound $NO_2^-$, $NO_3^-$, and HONO, as seen in Fig. 2a and reported in previous studies.[3,12–14,17,56–58]

The formation of additional products with peaks at 1280, 1584, and 1609 $cm^{-1}$ when the C8= SAM is present, accompanied by a decrease in the $-CH_2-$ and =CH peaks (Fig. 2b), indicate that some of the surface-bound products of the $NO_2$ chemistry react with the attached organic. Since this occurs in the dark as well as upon photolysis, the oxidizing species that initiates the chemistry is likely to be one or more of the intermediates and/or products in Reactions (2)–(4). We propose that $NO^+$ initiates the oxidation *via* two pathways: addition of $NO^+$ to the double bond directly, or conversion of $NO^+$ to $N_2O_3$, which in turn adds to the double bond,[71]

$$R_2C{=}CR_2 + NO^+ \rightarrow R_2C(NO)–C^+R_2 \quad (6)$$

$$R_2C{=}CR_2 + N_2O_3 \rightarrow R_2C(NO)–C(NO_2)R_2 \quad (7)$$

where R represents any organic group. By analogy to aqueous systems, the mechanism of dinitrogen trioxide formation in these experiments can stem from the reaction of $NO^+$ with basic surface sites on alumina to form an adsorbed nitrito species, which subsequently reacts with nitrite ion to give $N_2O_3$:[71]

$$NO^+ + O^-\text{-alumina} \rightarrow \text{ONO-alumina} \quad (8)$$

$$\text{ONO-alumina} + NO_2^- \rightarrow N_2O_3 + O^-\text{-alumina} \quad (9)$$

While adsorbed $N_2O_3$ was not observed in experiments when $H_2O$ was present, an appreciable amount (indicated by a broad band centered at 1950 $cm^{-1}$) did form during exposures of alumina to $NO_2$ under dry conditions, in agreement with previous studies.[17]

The carbocations formed in reaction (6) may undergo a number of reactions, including the addition of anions or the elimination of a proton to generate an alkene.[72] Scheme 1 shows a sequence of reactions that leads to the formation of a nitro group ($R_2C–NO_2$) which is a precursor to a nitronate ($R_2C{=}NO_2^-$)[72,73] that is likely chelated to $Al^{3+}$ sites on the surface. Nitronates are known to have strong peaks that correspond to the 1280, 1584 and 1609 $cm^{-1}$ bands observed here.[53,74] As shown in Scheme 1, addition of $NO^+$ to a double bond forms a nitroso compound ($R_2C–NO$) that can generate a nitrile ($RC{\equiv}N$) *via* dehydration of an oxime intermediate; the stretching vibration of the $–C{\equiv}N$ group is typically in the range of 2200–2600 $cm^{-1}$, and we assign the weak peak at 2262 $cm^{-1}$ (Fig. 3a,b) to a nitrile.[53,75] While peaks in the 2250 $cm^{-1}$ range have been assigned to $NO^+$ in previous studies,[17,68–70,56,76] the peak at 2262 $cm^{-1}$ only appeared when the organic coating was present, suggesting it is likely due to an organic product such as a nitrile. It is also possible that this peak belongs to an isocyanate (RNCO) species.[77,78] However, it is not possible to distinguish between these two possibilities spectroscopically, but mechanistically, the formation of nitriles is more reasonable.

An alternative mechanism for the formation of nitroso-organic products may be the activation of a methylene group by its interaction with a basic site on the alumina surface. The resulting carbanion may then be nitrosated by $NO^+$ on the surface:[71,72]

$$R_3C–H + O^-\text{-alumina} \rightarrow R_3C:^- + \text{HO-alumina} \quad (10)$$

$$R_3C:^- + NO^+ \rightarrow R_3C–NO \quad (11)$$

The formation of allylic carbanions coordinated to $Al^{3+}$ in tetrahedral vacancies has been observed in studies of propene

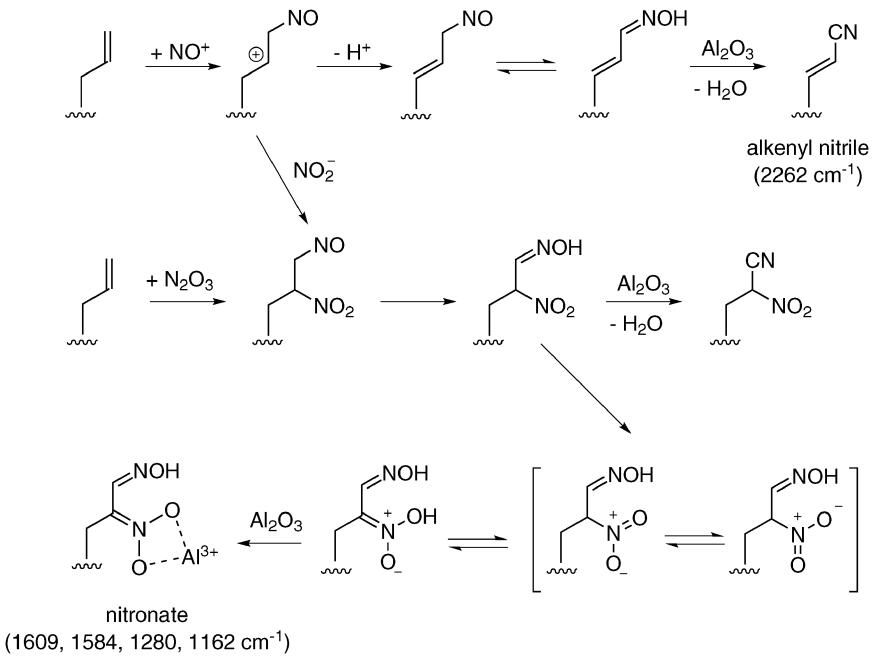


**Scheme 1** Thermal reactions leading to organo-nitrogen products.

 

on alumina or other metal oxide surfaces.[79–81] It is also possible that the proximity of the hydrocarbon chain to acidic sites on the alumina surface could promote reactions leading to carbocations that react similarly to those formed in reaction (6).[82–84] In short, the products formed in Fig. 3a are likely a result of alumina-mediated reactions such as (6)–(11) that activate the hydrocarbon chain toward reaction with adsorbed $NO_x$ species.

While there is evidence from solution phase reactions that the ion pair $NO^+NO_3^-$ reacts with alkenes to give organo-nitrosonitrates,[85,86] this should lead to a strong absorption band in the 1615–1660 $cm^{-1}$ region due to the asymmetric $NO_2$ stretch as well as in the 1250–1300 $cm^{-1}$ region due to the symmetric $NO_2$ stretch. While there is a strong band at 1280 $cm^{-1}$ in Fig. 3a, a band in the asymmetric $NO_2$ region only appears after photolysis (see below). Hence direct reaction of the ion pair with the alkene seems unlikely in the present experiments, perhaps due to separation of the ions and their strong adsorption on the alumina surface.

During photolysis, the band at 1228 $cm^{-1}$ assigned to HONO decreases as expected since HONO is known to photolyze rapidly[24] to generate OH and NO:

$$HONO + h\nu \rightarrow OH + NO \quad (9)$$

Nitrite ions also photolyze above 300 nm[19,20] and form OH radicals if water is available:

$$NO_2^- + h\nu \rightarrow NO + O^- \quad (10)$$

$$O^- + H_2O \rightarrow OH + HO^- \quad (11)$$

In either case, NO is generated, which accounts for the mass spectral peak at $m/z$ 30 during irradiation (Fig. 4a). From diffuse reflection UV-vis absorption measurements it was previously reported that the $\pi^* \leftarrow n$ transition of nitrate adsorbed to alumina surfaces is centered at 275 nm,[13] blue-shifted from 310 nm observed for aqueous sodium nitrate.[19] Thus, there is poor overlap of the lamp emission spectrum with the absorption spectrum of adsorbed nitrate. This is consistent with our observation that nitrate does not photolyze further under the conditions of these experiments.

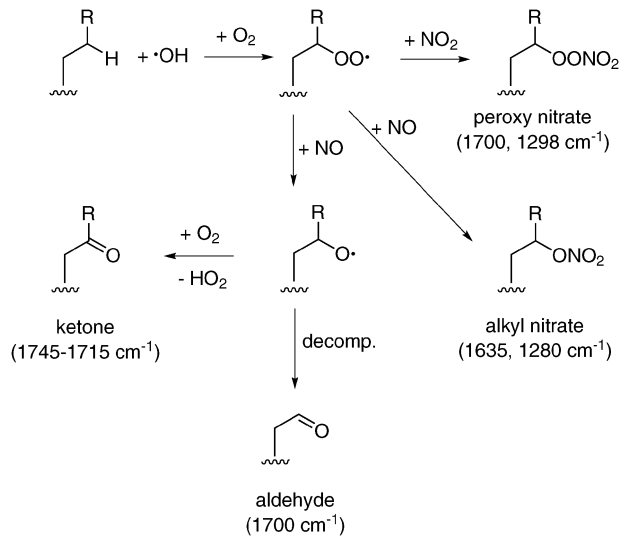


**Scheme 2** Mechanism of C8= photooxidation on alumina in the presence of adsorbed $NO_x$.

Scheme 2 shows the mechanism of oxidation of the alkyl chain initiated by OH, which leads to the formation of organic nitrates, peroxy nitrates, aldehydes, and ketones. The peak at 1638 $cm^{-1}$ that appears in the photolysis experiments (Fig. 3b) is assigned to $RONO_2$,[53,87] and is accompanied by a peak at 1280 $cm^{-1}$, which is overlapped by that from nitronate species. The combination of peaks at 1700 $cm^{-1}$ and 1298 $cm^{-1}$ suggests formation of a peroxy nitrate ($ROONO_2$),[87] although as discussed below, there may be a contribution from a carbonyl group at 1700 $cm^{-1}$.

While OH radicals may attack at either the terminal alkene group or along the alkyl chain, the relatively small loss of the $=CH_2$ moiety (Fig. 3b) suggests that the alkyl chain is the main point of attack *via* H-abstraction. This is not surprising since the C=C group is at the far end of the chain, distant from the surface that generates and holds the reactive intermediates. Similar conclusions were reached by Karagulian *et al.*[41] in their studies of the photooxidation of partially saturated phospholipids adsorbed to $NaCl/NaNO_2$ salt mixtures.

The production of gas phase CO and $CO_2$ (Fig. 4a) is somewhat surprising. Although oxidation of hydrocarbons will lead to these products and has been observed in the reaction of gas-phase $O_3$ and OH with organic self-assembled monolayers on quartz,[88–90] it requires a number of secondary reactions. However, here the experiments show that CO and $CO_2$ are generated immediately on photolysis. We have observed in unrelated studies that $O_3$ is generated from photolysis of as-of-yet unidentified oxides of nitrogen bound to stainless steel surfaces. If $O_3$ were also generated in the present system, oxidation of the double bond would lead to an aldehyde and a one-carbon Criegee intermediate HCHOO, which is known to decompose to CO and $CO_2$.[24] In this case, the 1700 $cm^{-1}$ infrared band (Fig. 3b) may also include a contribution from aldehydes arising from ozonolysis reactions.

## Atmospheric implications

Hydrocarbons are oxidized by surface-bound oxides of nitrogen formed in the uptake and hydrolysis of $NO_2$ on alumina, which is used here as a proxy for airborne dust, soils, and building materials. This occurs not only during irradiation, but also in the dark at approximately half the rate driven by photolysis. This chemistry will lead to a variety of organonitrogen compounds being formed on dust particles, soils, and building materials, and to the regeneration of gaseous products such as NO, CO, $CO_2$ and potentially, some small organic molecules generated during the oxidation. The actinometer measurements indicate that in these experiments the light intensity in the 290–400 nm region is about three orders of magnitude larger than that at Earth's surface from an overhead sun.[24] Assuming the rate of the photochemical oxidation is proportional to the light intensity, this suggests that the photolysis reactions will be much slower in air than observed here, and that it is the thermal reactions that will actually be more important under atmospheric conditions.

In short, oxides of nitrogen and organics are not only removed by adsorption on the surfaces of airborne dust particles, soils, and building materials, but these surfaces provide a medium for their further reactions, both in the dark and under solar irradiation.

## Summary

Gas phase $NO_2$ reacts with an alkene self-assembled monolayer on $\gamma$-$Al_2O_3$ that had been exposed to water vapor both in the dark and under irradiation with wavelengths above 290 nm. Unique organo-nitrogen products such as nitronates ($R_2C{=}NO_2^-$) and possibly nitriles (*e.g.*, RCH=CHCN) were identified as products in the dark. Under irradiation, organic nitrates and possibly peroxynitrates and/or carbonyl compounds are formed, and gas-phase NO, CO, and $CO_2$ are generated. This chemistry suggests that both thermal and photochemical reactions of nitrogen oxides with organics on surfaces should be considered in models of processes occurring in the lower atmosphere.

## Acknowledgements

We thank Ja Hun Kwak for XRD analysis of the alumina used in this study, and Alan Joly and Paul Gassman for assistance with emission spectroscopy. Christopher Dilbeck, Mark Engelhardt, Theresa McIntire, Samar Moussa and Zihua Zhu are gratefully acknowledged for helpful discussions. J.D.R. is grateful to the National Science Foundation for fellowship support under CHE-0836070. This work was carried out at AirUCI, an Environmental Molecular Sciences Institute funded by the National Science Foundation (Grant # CHE-0431312 and 0909227) and at the Environmental Molecular Sciences Laboratory (EMSL) at Pacific Northwest National Laboratory (PNNL). The EMSL is a national scientific user facility supported by the U.S. DOE, Office of Science/Biological and Environmental Research. PNNL is a multiprogram national laboratory operated for the U.S. DOE by Battelle Memorial Institute under Contract DE-AC06-76RLO 1830.

## References

1 IPCC, Climate Change 2007: The Physical Science Basis. Contribution of Working Group I to the Fourth Assessment Report of the Intergovernmental Panel on Climate Change, Cambridge University Press, Cambridge, United Kingdom, 2007.
2 J. M. Prospero, *Proc. Natl. Acad. Sci. U. S. A.*, 1999, **96**, 3396–3403.
3 C. R. Usher, A. E. Michel and V. H. Grassian, *Chem. Rev.*, 2003, **103**, 4883–4940.
4 P. R. Buseck and M. Posfai, *Proc. Natl. Acad. Sci. U. S. A.*, 1999, **96**, 3372–3379.
5 M. Kanakidou, *et al.*, *Atmos. Chem. Phys.*, 2005, **5**, 1053–1123.
6 T. Sandstrom and B. Forsberg, *Epidemiology*, 2008, **19**, 808–809.
7 F. J. Dentener, G. R. Carmichael, Y. Zhang, J. Lelieveld and P. J. Crutzen, *J. Geophys. Res.*, 1996, **101**, 22869–22889.
8 R. M. E. Diamant, *The Chemistry of Building Materials*, Business Books Limited, London, 1970.
9 K.-P. Hinz, A. Trimborn, E. Weingertner, S. Henning, U. Baltensperger and B. Spengler, *J. Aerosol Sci.*, 2005, **36**, 123–145.
10 D. M. Murphy and D. S. Thomson, *J. Geophys. Res.*, 1997, **102**, 6353–6368.
11 A. Tabazadeh, M. Z. Jacobson, H. B. Singh, O. B. Toon, J. S. Lin, R. B. Chatfield, A. N. Thakur, R. W. Talbot and J. E. Dibb, *Geophys. Res. Lett.*, 1998, **25**, 4185–4188.
12 A. L. Goodman, T. M. Miller and V. H. Grassian, *J. Vac. Sci. Technol., A*, 1998, **16**, 2585–2590.
13 T. M. Miller and V. H. Grassian, *Geophys. Res. Lett.*, 1998, **25**, 3835.
14 E. Ozensoy, C. H. F. Peden and J. Szanyi, *J. Phys. Chem. A*, 2005, **109**, 15977–15984.
15 G. M. Underwood, C. H. Song, M. Phadnis, G. R. Carmichael and V. H. Grassian, *J. Geophys. Res.*, 2001, **106**, 18055–18066.
16 B. J. Finlayson-Pitts, L. M. Wingen, A. L. Sumner, D. Syomin and K. A. Ramazan, *Phys. Chem. Chem. Phys.*, 2003, **5**, 223–242.
17 J. Szanyi, J. H. Kwak, R. J. Chimentao and C. H. F. Peden, *J. Phys. Chem. C*, 2007, **111**, 2661–2669.
18 C. Börensen, U. Kirchner, V. Scheer, R. Vogt and R. Zellner, *J. Phys. Chem. A*, 2000, **104**, 5036–5045.
19 J. Mack and J. R. Bolton, *J. Photochem. Photobiol., A*, 1999, **128**, 1–13.
20 H. Herrmann, *Phys. Chem. Chem. Phys.*, 2007, **9**, 3935–3964.
21 J. Schuttlefield, G. Rubasinghege, M. El-Maasawi, J. Bone and V. H. Grassian, *J. Am. Chem. Soc.*, 2008, **130**, 12210–12211.
22 G. Rubasinghege and V. H. Grassian, *J. Phys. Chem. A*, 2009, **113**, 7818–7825.
23 J. Baltrusaitis, P. M. Jayaweera and V. H. Grassian, *Phys. Chem. Chem. Phys.*, 2009, **11**, 8295–8305.
24 B. J. Finlayson-Pitts and J. N. Pitts, Jr., *Chemistry of the Upper and Lower Atmosphere—Theory, Experiments, and Applications*, Academic Press, San Diego, 2000.
25 A. M. Winer and H. W. Biermann, *Res. Chem. Intermed.*, 1994, **20**, 423–445.
26 J. Stutz, B. Alicke, R. Ackermann, A. Geyer, S. H. Wang, A. B. White, E. J. Williams, C. W. Spicer and J. D. Fast, *J. Geophys. Res.*, 2004, **109**, D03307.
27 J. Stutz, B. Alicke and A. Neftel, *J. Geophys. Res.*, 2002, **107**, 8192.
28 S. Wang, R. Ackermann, C. W. Spicer, J. D. Fast, M. Schmeling and J. Stutz, *Geophys. Res. Lett.*, 2003, **30**, 1595.
29 L. M. Russell, S. F. Maria and S. C. B. Myneni, *Geophys. Res. Lett.*, 2002, **29**, 1779.
30 A. H. Falkovich, E. Ganor, Z. Levin, P. Formenti and Y. Rudich, *J. Geophys. Res.*, 2001, **106**, 18029–18036.
31 A. H. Falkovich, G. Schkolnik, E. Ganor and Y. Rudich, *J. Geophys. Res.*, 2004, **109**, D02208.
32 M. L. Diamond, S. E. Gingrich, K. Fertuck, B. E. McCarry, G. A. Stern, B. Billeck, B. Grift, D. Brooker and T. D. Yager, *Environ. Sci. Technol.*, 2000, **34**, 2900–2908.
33 S. E. Gingrich, M. L. Diamond, G. A. Stern and B. E. McCarry, *Environ. Sci. Technol.*, 2001, **35**, 4031–4037.
34 E. M. Hodge, M. L. Diamond, B. E. McCarry, G. A. Stern and P. A. Harper, *Arch. Environ. Contam. Toxicol.*, 2003, **44**, 421–429.
35 B. Lam, M. L. Diamond, A. J. Simpson, P. A. Makar, J. Truong and N. A. Hernandez-Martinez, *Atmos. Environ.*, 2005, **39**, 6578–6586.
36 Q. T. Liu, R. Chen, B. E. McCarry, M. L. Diamond and B. Bahavar, *Environ. Sci. Technol.*, 2003, **37**, 2340–2349.
37 A. J. Simpson, B. Lam, M. L. Diamond, D. J. Donaldson, B. A. Lefebvre, A. Q. Moser, A. J. Williams, N. I. Larin and M. P. Kvasha, *Chemosphere*, 2006, **63**, 142–152.
38 N. O. A. Kwamena, J. P. Clarke, T. F. Kahan, M. L. Diamond and D. J. Donaldson, *Atmos. Environ.*, 2007, **41**, 37–50.
39 D. J. Donaldson and K. T. Valsaraj, *Environ. Sci. Technol.*, 2010, **44**, 865–873.
40 F. Karagulian, C. W. Dilbeck and B. J. Finlayson-Pitts, *J. Am. Chem. Soc.*, 2008, **130**, 11272–11273.
41 F. Karagulian, C. W. Dilbeck and B. J. Finlayson-Pitts, *J. Phys. Chem. A*, 2009, **113**, 7205–7212.
42 Y. Rudich, *Chem. Rev.*, 2003, **103**, 5097–5124.
43 Y. Rudich, N. M. Donahue and T. F. Mentel, *Annu. Rev. Phys. Chem.*, 2007, **58**, 321–352.
44 A. R. Ravishankara, *Science*, 1997, **276**, 1058–1065.
45 S. G. Moussa and J. Finlayson-Pitts Barbara, *Phys. Chem. Chem. Phys.*, 2010, **12**, 9419.
46 M. Z. Rong, Q. L. Ji, M. Q. Zhang and K. Friedrich, *Eur. Polym. J.*, 2002, **38**, 1573–1582.

 

47 A. A. Yasseri, N. P. Kobayashi and T. I. Kamins, *Appl. Phys. A: Mater. Sci. Process.*, 2006, **84**, 1–5.
48 A. W. Adamson and A. P. Gast, *Physical Chemistry of Surfaces*, John Wiley & Sons, Inc., New York, 1997.
49 W. K. Hall, H. P. Leftin, F. J. Cheselske and D. E. O'Reilly, *J. Catal.*, 1963, **2**, 506–517.
50 J. N. Pitts Jr., J. K. S. Wan and E. A. Schuck, *J. Am. Chem. Soc.*, 1964, **86**, 3606–3610.
51 Y. Dubowski, J. Vieceli, D. J. Tobias, A. Gomez, A. Lin, S. A. Nizkorodov, T. M. McIntire and B. J. Finlayson-Pitts, *J. Phys. Chem. A*, 2004, **108**, 10473–10485.
52 S. G. Moussa, T. M. McIntire, M. Szori, M. Roeselova, D. J. Tobias, R. L. Grimm, J. C. Hemminger and B. J. Finlayson-Pitts, *J. Phys. Chem. A*, 2009, **113**, 2060–2069.
53 G. Socrates, *Infrared and Raman Characteristic Group Frequencies*, John Wiley & Sons, Chinchester, 2001.
54 R. Maoz and J. Sagiv, *J. Colloid Interface Sci.*, 1984, **100**, 465–496.
55 A. L. Kiselev, *Infrared Spectra of Surface Compounds*, John Wiley & Sons, New York, 1975.
56 K. I. Hadjiivanov, *Catal. Rev. Sci. Eng.*, 2000, **42**, 71–144.
57 J. Baltrusaitis, J. Schuttlefield, J. H. Jensen and V. H. Grassian, *Phys. Chem. Chem. Phys.*, 2007, **9**, 4970–4980.
58 G. M. Underwood, T. M. Miller and V. H. Grassian, *J. Phys. Chem. A*, 1999, **103**, 6184–6190.
59 T. Venkov, K. Hadjiivanov and D. Klissurski, *Phys. Chem. Chem. Phys.*, 2002, **4**, 2443–2448.
60 R. H. Kagann and A. G. Maki, *J. Quant. Spectrosc. Radiat. Transfer*, 1983, **30**, 37.
61 L. Khriachtchev, J. Lundell, E. Isoniemi and M. Räsänen, *J. Chem. Phys.*, 2000, **113**, 4265–4273.
62 S. E. Stein, "Mass Spectra", in *NIST Chemistry WebBook*, NIST Standard Reference Database Number 69, ed. P. J. Linstrom and W. G. Mallard, National Institute of Standards and Technology, Gaithersburg, MD, 20899.
63 M. Cwiertny David, A. Young Mark and H. Grassian Vicki, *Annu. Rev. Phys. Chem.*, 2008, **59**, 27–51.
64 J. Vieceli, O. L. Ma and D. J. Tobias, *J. Phys. Chem. A*, 2004, **108**, 5806–5814.
65 J. Dai, Z. Li, J. Jin, Y. Shi, J. Cheng, J. Kong and S. Bi, *Biosens. Bioelectron.*, 2009, **24**, 1074–1082.
66 Y. Miller, B. J. Finlayson-Pitts and R. B. Gerber, *J. Am. Chem. Soc.*, 2009, **131**, 12180–12185.
67 A. L. Goodman, G. M. Underwood and V. H. Grassian, *J. Phys. Chem. A*, 1999, **103**, 7217–7223.
68 J. Wang and B. E. Koel, *J. Phys. Chem. A*, 1998, **102**, 8573–8579.
69 J. Wang and B. E. Koel, *Surf. Sci.*, 1999, **436**, 15–28.
70 S. Hellebust, T. Roddis and J. R. Sodeau, *J. Phys. Chem. A*, 2007, **111**, 1167–1171.
71 D. L. H. Williams, *Nitrosation*, Cambridge University Press, Cambridge, 1988.
72 J. March, *Advanced Organic Chemistry: Reactions, Mechanisms, and Structure*, John Wiley & Sons, New York, 1992.
73 E. Breuer, H. G. Aurich and A. Nielsen, *Nitrones, Nitronates, and Nitroxides*, John Wiley & Sons, Inc., New York, 1989.
74 D. E. H. Jones and J. L. Wood, *J. Chem. Soc. A*, 1966, 1448–1453.
75 N. W. Hayes, W. Grünert, G. J. Hutchings, R. W. Joyner and E. S. Shpiro, *J. Chem. Soc., Chem. Commun.*, 1994, 531–532.
76 Y. Song, R. J. Hemley, Z. Liu, M. Somayazulu, H.-K. Mao and D. R. Herschbach, *J. Chem. Phys.*, 2003, **119**, 2232–2240.
77 N. W. Hayes, R. W. Joyner and E. S. Shpiro, *Appl. Catal., B*, 1996, **8**, 343–363.
78 T. Szailer, J. H. Kwak, D. H. Kim, J. C. Hanson, C. H. F. Peden and J. Szanyi, *J. Catal.*, 2006, **239**, 51–64.
79 G. Busca, E. Finocchio, V. Lorenzelli, M. Trombetta and A. Rossini, *J. Chem. Soc., Faraday Trans.*, 1996, **92**, 4687–4693.
80 M. Trombetta, G. Busca, S. A. Rossini, V. Piccoli and U. Cornaro, *J. Catal.*, 1997, **168**, 334–348.
81 A. A. Davydov, *Infrared Spectroscopy of Adsorbed Species on the Surface of Transition Metal Oxides*, John Wiley & Sons, Inc., New York, 1990.
82 C. S. John, C. Kemball, R. C. Paterson and R. A. Rajadhyaksha, *J. Chem. Soc., Chem. Commun.*, 1977, 894–896.
83 J. Nomura and H. Shima, *J. Jpn. Pet. Inst.*, 2008, **51**, 274–286.
84 C.-C. Hwang and C.-Y. Mou, *J. Phys. Chem. C*, 2009, **113**, 5212–5221.
85 E. F. J. Duynstee, J. G. H. M. Housmans, W. Voskuil and J. W. M. Berix, *Recueil des Travaux Chimiques des Pays-Bas*, 1973, **92**, 698–701.
86 J. B. Wilkes and R. G. Wall, *J. Org. Chem.*, 1980, **45**, 247–250.
87 J. M. Roberts, *Atmos. Environ.*, 1990, **24A**, 243–287.
88 E. R. Thomas, G. J. Frost and Y. Rudich, *J. Geophys. Res.*, 2001, **106**, 3045–3056.
89 M. J. Molina, A. V. Ivanov, S. Trakhtenberg and L. T. Molina, *Geophys. Res. Lett.*, 2004, **31**.
90 A. Vlasenko, I. J. George and J. P. D. Abbatt, *J. Phys. Chem. A*, 2008, **112**, 1552–1560.